

# Rapid Prototyping of Nanofluidic Systems Using Size-Reduced Electrospun Nanofibers for Biomolecular Analysis

Seung-min Park, Yun Suk Huh, Kylan Szeto, Daniel J. Joe, Jun Kameoka, Geoffrey W. Coates, Joshua B. Edel, David Erickson, and Harold G. Craighead\*

**B**iomolecular transport in nanofluidic confinement offers various means to investigate the behavior of biomolecules in their native aqueous environments, and to develop tools for diverse single-molecule manipulations. Recently, a number of simple nanofluidic fabrication techniques has been demonstrated that utilize electrospun nanofibers as a backbone structure. These techniques are limited by the arbitrary dimension of the resulting nanochannels due to the random nature of electrospinning. Here, a new method for fabricating nanofluidic systems from size-reduced electrospun nanofibers is reported and demonstrated. As it is demonstrated, this method uses the scanned electrospinning technique for generation of oriented sacrificial nanofibers and exposes these nanofibers to harsh, but isotropic etching/heating environments to reduce their cross-sectional dimension. The creation of various nanofluidic systems as small as 20 nm is demonstrated, and practical examples of single biomolecular handling, such as DNA elongation in nanochannels and fluorescence correlation spectroscopic analysis of biomolecules passing through nanochannels, are provided.

## 1. Introduction

Nanofluidic systems provide promising solutions for detection, sensing and biomolecular handling in single molecule environments due to their extremely small confinement. Many research groups have demonstrated distinctive

bioanalytical applications such as a biomolecular preconcentrator,<sup>[1,2]</sup> nanogap detector<sup>[3,4]</sup> and single biomolecule manipulation device<sup>[5,6]</sup> with continued work towards practical analytical applications.<sup>[7–10]</sup> However, important issues remain, especially concerning the intricacy of the fabrication processes involved, which limit rapid prototyping

---

Dr. S.-m. Park,<sup>[+]</sup> K. Szeto, Prof. H. G. Craighead  
School of Applied and Engineering Physics  
Cornell University  
205 Clark Hall, Ithaca, NY 14853, USA  
E-mail: hgc1@cornell.edu

Dr. Y. S. Huh,<sup>[++]</sup> Prof. D. Erickson  
Sibley School of Mechanical and Aerospace Engineering  
Cornell University  
Ithaca, NY 14853, USA

D. J. Joe  
School of Electrical and Computer Engineering  
Cornell University  
Ithaca, NY 14853, USA

Prof. J. Kameoka  
Department of Electrical and Computer Engineering  
Texas A&M University, USA

Prof. G. W. Coates  
Department of Chemistry and Chemical Biology  
Cornell University  
Ithaca, NY 14853, USA

Dr. J. B. Edel  
Department of Chemistry and Institute of Biomedical Engineering  
Imperial College London  
SW7 2AZ, London, UK

[+] Current Address: Biomolecular Nanotechnology Center, Berkeley Sensor and Actuator Center, Department of Bioengineering, University of California at Berkeley, Berkeley, CA 94720, USA

[++] Current Address: Division of Materials Science, Korea Basic Science Institute, Daejeon, 305-333, South Korea

DOI: 10.1002/smll.201000884

and mass-production of nanofluidic systems. Significant progress has been made in developing techniques suitable for simple fabrication of nanofluidic systems; for example, nanofabrication methods based on soft lithography (e.g. wrinkling,<sup>[11]</sup> cracking<sup>[12]</sup> and collapsing<sup>[6]</sup> nature of the elastomeric material) or sacrificial nanofiber template methods using electrospinning.<sup>[13–16]</sup>

Recently, a growing number of bioanalytical research has incorporated electrospun nanofibers<sup>[17–22]</sup> due to their cost effectiveness, ease of fabrication and material selectivity. In particular, various methods to form nanochannels based on electrospinning have been introduced. For instance, Wang et al.<sup>[16]</sup> utilized a coaxial electrospinning technique to fabricate nanochannels. Previously, Czaplewski et al.<sup>[14]</sup> presented a method for fabricating nanochannels with removal of glass-covered sacrificial nanofibers. Other work by Verbridge et al.<sup>[15]</sup> showed the fabrication of suspended nanochannels spanning a trench with the use of sputtered-glass encapsulated sacrificial nanofibers. In that work the mechanical quality factor and the resonant frequency of the resulting nanochannel were also reported. However, while these previous works<sup>[14–16]</sup> based on electrospinning methods showed that nanochannels could be filled with fluorescent analytes, no further molecular manipulation (e.g. measurements of the electrophoretic mobility of biomolecules, elongation of macromolecules, etc.) in the nanochannels has been made.

In this study, we demonstrate a method by which heat depolymerizable polycarbonate (HDPC) nanofibers can be employed as a dimension-controllable backbone of a nanofluidic system. Here, we show that a nanofluidic system as small as 20 nm can be made by simple post-treatments to the backbone nanofibers using heat or plasma. To extend nanofluidic applications to the level of the single biomolecular manipulation, we demonstrate fluorescence correlation spectroscopy (FCS) in the nanochannels. As it is a robust tool for the characterization of biomolecules, the FCS provides dynamic molecular properties such as the diffusion constant and speed of an analyte driven by an external force, especially in nanochannels with dimensions comparable to or even smaller than the optical excitation volume.<sup>[23]</sup> We also demonstrate the manipulation of large DNA molecules confined in the nanochannels for possible genomic applications.

## 2. Materials and Methods

### 2.1. Sacrificial Electrospun Nanofiber and Nanochannel Formation

Glass substrates including commercially available and transparent cover glasses or fused silica (Esco Products Inc., Oak Ridge, NJ) were selected as target substrates because they provide low background for fluorescent detection, high transparency for use on an inverted microscope, and an insulation layer for electrical applications. Spin-on-glasses (SOG) with film thicknesses of 200 nm (IC1-200) and 500 nm

(DC4-500) were purchased from Futurrex (Franklin, NJ). Chlorobenzene was provided by Sigma-Aldrich (St. Louis, MO). HDPC (Heat Depolymerizable Polycarbonate) was synthesized by reacting cyclohexene oxide and carbon dioxide with a homogeneous, zinc-based catalyst.<sup>[24,25]</sup> In order to create nanofibers as a sacrificial template, electrospinning (the process of creating nanofibers from a polymer solution using an electrically forced fluid jet<sup>[26,27]</sup>) was employed. The scanned electrospinning method<sup>[28]</sup> was used where the collecting substrate is rotated through the jet to produce oriented nanofiber arrays. The electrospinning setup is illustrated in Figure S1A of the Supporting Information. In this experiment, a 30% (by weight) HDPC ( $M_w = 54,000$ ) – chlorobenzene solution was prepared for the sacrificial template of the nanofluidic channels. Then, the electrospun HDPC fibers were deposited onto a glass chip, and spin-on-glass was spin-coated on top and allowed to cure for crosslinking at 200 °C. To make various nanochannel diameters, spin-on glasses with various film thicknesses of 200 nm (IC1-200) and 500 nm (DC4-500) were used. For smaller nanofibers up to 200 nm, we used a single 200 nm layer provided by IC1-200. For nanofibers up to 500 nm, we used a single 500 nm layer spun by DC4-500. Up to 1  $\mu\text{m}$ , two layers of 500 nm provided by DC4-500 were used. In detail, using a pipetter, the spin-on glass solution was dispensed on the surface. Then, the chip was spun at 2000 rpm for 40 seconds and baked on a hotplate at 200 °C. Next, the chip was cured at 80 °C for 5 min and then ramped up to 250 °C over 15 min for depolymerization of the polycarbonate backbone. Since the diameter of each electrospun nanofiber can vary greatly from tens of nanometers to micrometers, the above process (except for the curing and ramping steps) was repeated to ensure complete coverage of nanofibers resulting in up to a 1  $\mu\text{m}$  thick glass layer. The overall fabrication process for forming nanochannels is minutely demonstrated in **Figure 1**.

### 2.2. Analysis of Electrospun Nanofibers

Atomic force microscopy (AFM) (Dimension 3000; Veeco, CA) operated in tapping mode was used to investigate the dimension of electrospun nanofibers. The scan size ranged from 5  $\mu\text{m}$  ~ 20  $\mu\text{m}$ . In order to minimize convolution effects, the scan rate was fixed at 0.5 Hz. Artifacts from an AFM tip make height measurements more meaningful since the width of the nanofibers is misrepresented due to the combination of the AFM tip and sample geometries. Examples of AFM images are shown in **Figure 2** and an example of deconvoluted AFM images is presented in Figure S2.

To measure the cross-section of the nanochannels, completed chips were fractured orthogonal to the direction of the oriented nanochannels. For imaging purposes, nanofibers were electrospun onto a silicon/silicon oxide substrate. The nanochannel cross-section was imaged without any metal layer deposition, using a field emission scanning electron microscope (LEO 1550 FESEM (Keck SEM); Leo Electron Microscopy, UK). Selected images of the fractured cross-section are shown in **Figure 3**.

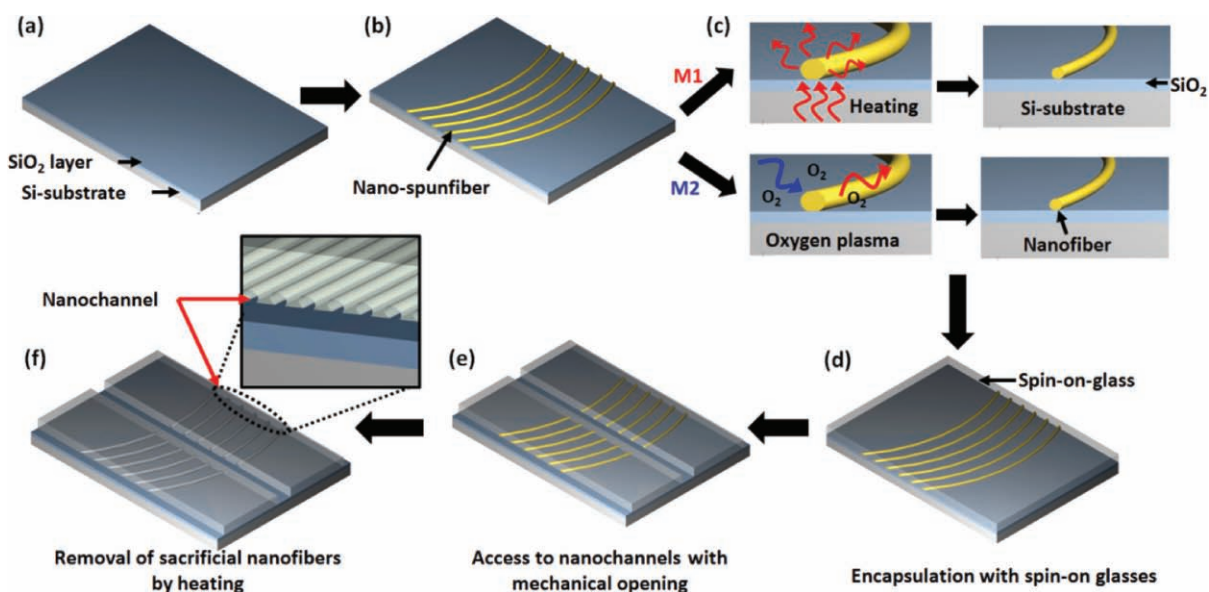


**Figure 1.** Schematic diagram of nanochannel formation with electrospun nanofibers. After the formation of electrospun nanofibers on the substrate, two types of post-treatments were employed in order to reduce the dimension of the nanochannels. Then, nanofibers were covered with spin-on-glass and removed by heat. Resulting nanochannels can be accessed by mechanically defined inlet ports.

### 2.3. T4-Bacteriophage DNA Preparation for Single-Molecule Manipulation in Nanochannels

169 kbp long T4-DNA was purchased from Wako (Richmond, VA). We labeled this DNA with bis-intercalating dye, YOYO-1 (Molecular Probes, Eugene, OR), and introduced it into the nanochannel, which was filled with filtered  $5\times$  tris-borate-EDTA (TBE) buffer (Sigma, St. Louis, MO)

at a concentration of  $50\text{ ng mL}^{-1}$ . This buffer contained 3% (v/v) polyvinylpyrrolidone (Sigma, St. Louis, MO), a surfactant to prevent adhesion of the specimen to the inner-surface of the nanochannels, and a 3% (v/v)  $\beta$ -mercaptoethanol (Sigma, St. Louis, MO) to decrease photobleaching. According to Mannion et al.,<sup>[29]</sup> the total contour length of T4-DNA with YOYO-1 is expected to be  $70.7\text{ }\mu\text{m}$ .

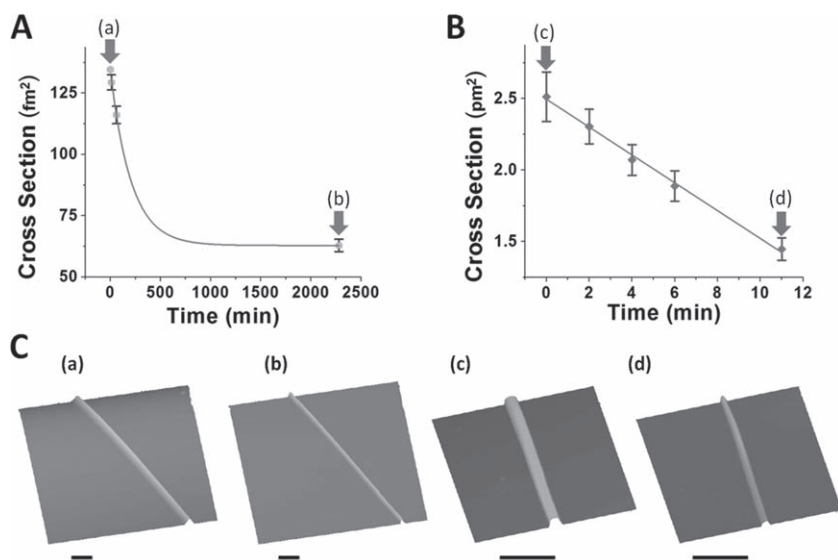


**Figure 2.** A) Plot of the dimension reduction of a nanofiber by heat. An exponential decay-like reduction was observed ( $R^2 = 0.9977$ ) due to solvent evaporation right after heating. B) Plasma etch effect on the cross-sectional reduction of the nanofiber. A significant linear relationship between the reduction and time was observed ( $R^2 = 0.9958$ ). C) AFM images for sacrificial nanofibers before and after heating ((a), (b)) and plasma etching ((c), (d)) recipe, respectively.  $40 \approx 50\%$  of dimension reduction was achieved. Because of the tip convolution effects, lateral dimensions of the nanofiber are exaggerated. (Scale bars,  $5\text{ }\mu\text{m}$ )

### 2.4. Fluorescence Correlation Spectroscopy

Fluorescence Correlation Spectroscopy (FCS) measurements were performed using a  $60\times 1.2$  numerical aperture (NA) water immersion objective lens (Olympus, Melville, NY). A detailed description of the FCS set up can be found in Figure S1B. Alexa Fluor 488-5-dUTP (Molecular Probes, Eugene, OR) was prepared by diluting in TBE (90 mM Tris-Borate, pH 8.0, 2 mM EDTA) to a final concentration of 100 nM. A surfactant with a 1% (v/v) Ige Pal (CA-630; Sigma-Aldrich, St. Louis, MO) and a 3% (v/v)  $\beta$ -mercaptoethanol was also added to prevent molecular adhesion and decrease photobleaching. The sample solution was pipetted into one reservoir while the other reservoir was kept empty to induce capillary filling of the nanochannel and prevent air bubbles. After 30 min of capillary filling, the other reservoir was also filled with the buffer solution. Gold wires contacting the solution in the reservoirs were used to apply an electric field over the

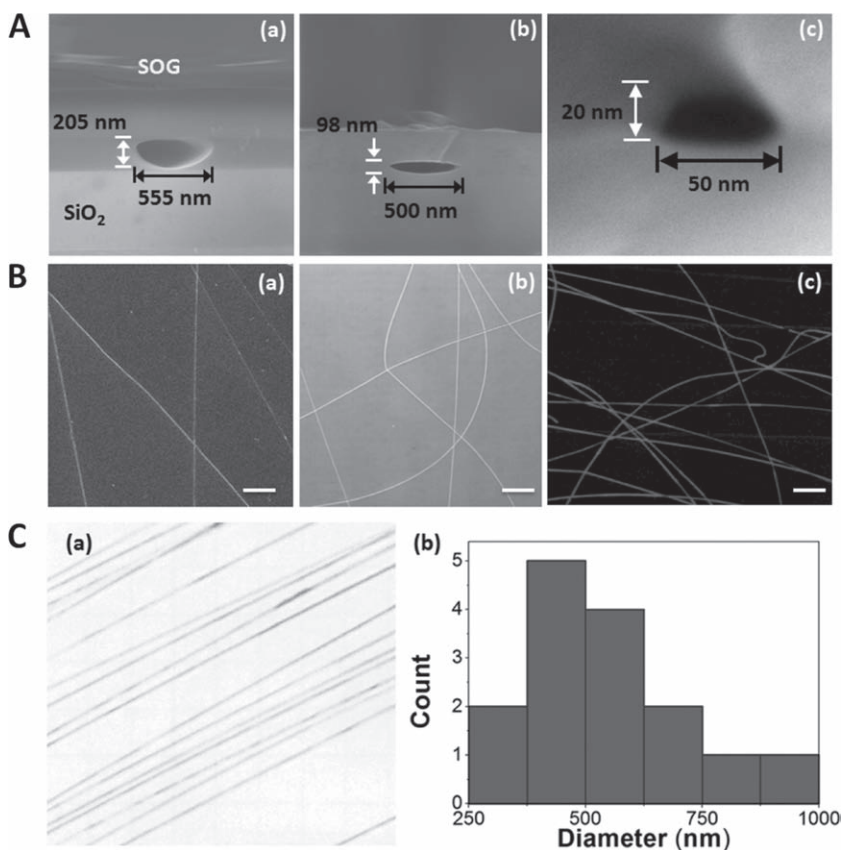


**Figure 3.** Scanning electron microscopy (SEM) image analysis of the nanochannels. A) Cross-sectional SEM image of nanochannels without the dimension reduction (a); SEM image of a low aspect ratio (1:5) nanochannel (b); cross-sectional SEM image of the channels after the dimension reduction (c). B) SEM image of electrospun nanofibers (a); optical image of random nanochannels after removal of sacrificial nanofibers (b); fluorescence image of nanochannels filled with a dye solution (c). (Scale bars, 5  $\mu\text{m}$ ) C) Optical image of nanofibers by the scanned electrospinning method (a); histogram of the diameter distribution (b).

nanochannels. To avoid generation of the triplet state population of fluorophores, we kept the laser intensities as low as 100  $\mu\text{W}$  minimizing the rate of photodestruction of the individual fluorescent molecules.<sup>[30]</sup>

### 3. Results and Discussion

#### 3.1. Nanochannel Formation and Characterization of Electrospun Nanofiber

Although slightly different from the solution used due to different molecular weight in previous work,<sup>[14]</sup> electrospinning of a 30% HDPC–chlorobenzene solution yielded consistent nanofibers (100 ~ 1000 nm) on the target substrate as shown in Figure 3B. Nanofibers by the scanned electrospinning method<sup>[28]</sup> were deposited on a substrate. As shown in Figure 3C, the deposited nanofibers were highly oriented in a concentric manner. Each fiber's angle was measured in order to calculate how parallel they were deposited. Their angles were within the standard deviation, 1.1° ( $N = 16$ ). Moreover, each diameter was also measured in order to analyze its distribution. Various

methods including SEM, AFM and optical microscopy were used and the diameters were obtained and analyzed. The Gaussian-like diameter distribution was confirmed as in Figure 3C. ( $N = 15$ ) The average diameter is  $503 \pm 167$  nm. In summary, as expected, the scanned electrospinning was able to lessen the random nature of electrospinning to a certain extent.

Two novel methods were used to reduce the diameter of sacrificial electrospun nanofibers. First, by directly heating the nanofibers under the glass transition temperature ( $T_g = 120$  °C) of HDPC, we expected that the nanofibers slowly sublime so that the total dimension of the nanofiber is reduced over time. While HDPC completely dissociates into a nontoxic vapor of monomer units when it is heated above 250 °C, it is believed that sublimation of HDPC will gradually take place near its glass transition temperature. The AFM micrographs in Figure 2A indicate that both dimensions including width and height were reduced after heating. 38 hours of heating at 110 °C resulted in approximately a 50% cross sectional reduction. The dimensions of the nanofibers (both width and height represented in the AFM micrographs) were reduced while their original shape was kept intact. It should be noted that the rate of reduction is greater during the first 10 min because residual solvent (e.g., chlorobenzene) in nanofibers starts to evaporate quickly as the ambient temperature approaches the glass transition temperature.

Secondly, it is well known that effective removal of certain polymers is possible with either oxygen plasma or UV-ozone processes. The etch rate of various polymers with the oxygen plasma can be found elsewhere.<sup>[31]</sup> Since HDPC is a member of the polycarbonate family, it is expected that HDPC nanofibers will react with oxygen plasma. The high energy plasma particles (radicals of O<sub>2</sub>) combine with organic material (C, H) to form carbon dioxide (CO<sub>2</sub>) or methane (CH<sub>4</sub>).<sup>[32]</sup> We discovered that a low power (7.16 W) oxygen plasma etch with a plasma cleaner (Harrick, Ithaca, NY), performed over the whole substrate at 500 mTorr, gave similar results in terms of reduction compared to the heating process described above. Moreover, the plasma etch took only several minutes instead of approximately 1.6 days required for the heating process. The isotropic nature of the oxygen plasma enabled nanofibers to hold their original shape after the etching process. It also provided a consistent ( $R^2 = 0.9977$ ) etch rate up to 12 min. AFM images taken before and after reduction treatments can be seen in Figure 2C, validating the uniformity of the reduction. For general use of this plasma process for more nanofiber materials, polyethylene oxide (PEO) nanofibers by the same electrospinning method were chosen for the test. Reduction of PEO nanofibers was also

investigated and correspondingly confirmed. After applying one minute oxygen plasma on the whole substrate, we were able to validate the overall and uniform reduction of PEO nanofibers as shown in Figure S3. It was also verified that the reduction rate of the PEO nanofibers is similar to that of the HDPC nanofibers. Therefore, we can extend this application of nanofibers reduction to the general organic materials used for electrospinning. For example, for the formation of the 3D fluidic vascular structure as demonstrated in Bellan et al.'s work,<sup>[21]</sup> this reduction technique can down-control the mean size of the vascular structure in that the backbone can be further reduced.

After the deposition and dimension-reduction of the nanofibers, a spin-on glass was spun over the substrate to create the nanochannels. The nanochannels were fabricated with various elliptical major and minor radii ranging from 20 ~ 500 nm depending on their original nanofiber sizes. Due to the out of plane contraction of the spin-on glass, all of the nanochannels fabricated by this method showed elliptical cross-section with minor axes perpendicular to the surface. By exerting a normal force, around 10 N cm<sup>-2</sup>, on the surface during the curing step, nanochannels with a lower aspect ratio (up to 1:5) were also obtained as can be seen in Figure 3A. In the end, these methods resulted in uniform glass tubes of elliptical cross-section with minor axis down to 20 nm, obtained by using plasma etched nanofibers.

In previous work,<sup>[14]</sup> after encapsulation with spin-on glasses, the capping layer was dry-etched down to the substrate using a CHF<sub>3</sub>/O<sub>2</sub> plasma chemistry in order to provide an entrance for accessing the nanochannels. This process requires the use of a photoresist layer as a mask and plasma chemistry to etch an entrance to the nanochannel. To simplify the process, we developed a mechanical method for opening the capping glass layer by scratching the surface with a razor blade instead of using lithographic tools. After curing and crosslinking of the glass layer, two razor blade scratches were made at the ends of the encapsulated nanofiber. Then, the whole substrate was heated to 250 °C for depolymerization. Finally, to access the nanofluidic network, PDMS gaskets (Culture well, Grace Bio-Lab, Bend, OR) were attached over the scratches and used as reservoirs for accessing the nanochannels. The remaining processes are described in detail elsewhere.<sup>[14]</sup> The accessibility to the nanochannel was confirmed by filling over the razor cut with a dye solution. In Figure S4, the nanochannel filled with the dye solution is depicted. Few collapse events of the inlet ports were observed so that most of the nanochannels were accessible after razor cuts were made. In summary, this process is able to replace existing technology and simplify the creation of nanofluidic systems.

### 3.2. Single-Molecule Manipulation in a Nanochannel

In order to examine the fluidic continuity of the formed nanochannels, we filled

them with a solution of 50 μM Rhodamine B in 50:50 isopropanol/water and imaged them using an optical microscope (Olympus IX-70 microscope; Olympus, Melville, NY). As shown in Figure 3, we were able to fill simple nanochannels as well as random nanofluidic networks. To demonstrate the practical application of these devices to single molecule analysis, we imaged individual DNA molecules in solution as they passed through the nanochannels. The nanochannel had two large reservoirs at the entrance provided by polydimethylsiloxane (PDMS) gaskets. When electrophoretically driven into the nanochannel, the T4 DNA molecule stretched to about 30 μm, which is ~40% of its full contour length. By the calculation provided before,<sup>[6,33]</sup> the observed contour length (~30 μm) of T4 DNA suggests that the confined nanochannel width is about 90 nm along one axis. We were also able to measure the speed of T4 DNA molecules by imaging the intensity fluctuation of DNA molecules as shown in Figure 4. We traced the endpoints of the molecule, and performed a linear fitting, which yielded the molecular speed (5 μm/sec) in the nanochannel with high correlation ( $R^2 = 0.9742$ ).

### 3.3. Single-Molecule Analysis with Fluorescence Correlation Spectroscopy

To demonstrate the confinement effect of these nanochannels, FCS was performed on a nanochannel approximately 250 nm across. FCS curves from the analyte confined in the nanochannel shifted as applied electric fields increased, shown in Figure 5. Each curve represents the average of 5 consecutive 30-second measurements. Assuming a Gaussian profile of the input laser, we fit the curves to the one dimensional autocorrelation function as given by Foquet et al.<sup>[23]</sup>

$$G(\tau) = \frac{1}{N} \frac{1}{\sqrt{1 + \frac{\tau}{\tau_d}}} \exp \left\{ - \left( \frac{\tau}{\tau_f} \right)^2 \frac{1}{\sqrt{1 + \frac{\tau}{\tau_d}}} \right\} \quad (1)$$

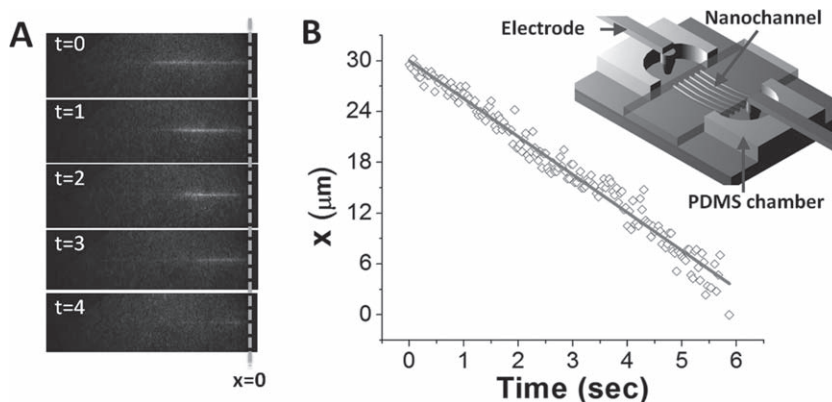
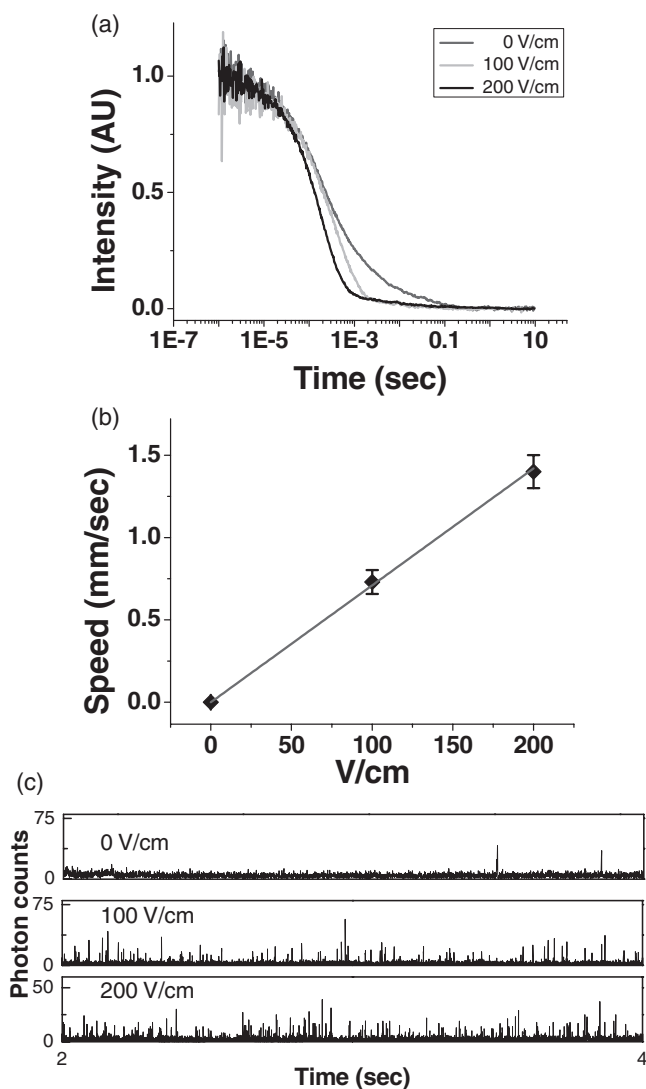


Figure 4. A) Electrophoretic migration of an elongated 169 kbp long T4-DNA in the nanochannel by 5 V/cm (Time interval between frames is one second.). B) Plot of the left-endpoint of the T4-DNA molecule stretched in the nanochannel. The molecule was driven linearly by the external electric field. ( $R^2 = 0.9743$ ) The estimated molecule speed in the nanochannel is slightly less than 5 μm s<sup>-1</sup>.



**Figure 5.** FCS analysis of Alexa Fluor 488-5-dUTP in 3 different electric fields. Correlation curves at (A)  $0 \text{ V cm}^{-1}$  (pure diffusion),  $100 \text{ V cm}^{-1}$ ,  $200 \text{ V cm}^{-1}$  are shown. Each curve is the average of 5 consecutive measurements (in 30 s). All these curves are fit into the Equation (1). B) The analyte speed in the nanochannel according to its applied field. Speed as high as  $1.4 \text{ mm s}^{-1}$  was obtained and proportional to the field. C) Photon burst scans in 3 different electric fields. With increasing the electric field, the events of the molecule passing through the focal volume increase proportionally.

where  $\tau_d$  accounts for the diffusion time,  $N$  for the average number of molecules, and,  $\tau_f$  for the flow time in the confined volume driven by the electric field. The flow speed  $v$  of the molecule can be calculated from the relation  $v = 2\omega/\tau_f$ , where  $\omega$  is the radius of the laser beam spot. The  $e^{-2}$  focal volume radius,  $\omega_x = 264 \text{ nm}$ , was obtained by using the equation,  $\omega_x = \sqrt{4D\tau_d}$ , where  $D$  represents the diffusion coefficient ( $2.1 \times 10^{-6} \text{ cm}^2 \text{ s}^{-1}$ )<sup>[23]</sup> of Alexa Fluor 488-5-2'-Deoxyuridine 5'-Triphosphate (dUTP) and accounts for the obtained parameter for the fit (Equation (1)). After the curves were acquired from the FCS experiment, a non-linear least-squares algorithm was used to fit the curves. The confined  $e^{-2}$  volume ( $528 \text{ nm}$  long cylinder with a radius of  $125 \text{ nm}$ ) created by the laser was around  $2.6 \times 10^{-20} \text{ m}^3$ .

Theoretically, the number of molecules in this confined volume with  $100 \text{ nM}$  solution should be around 1.56 according to the relation,  $N = CV_{\text{eff}}$  where  $C$  stands for the concentration and  $V_{\text{eff}}$  for the effective observation volume. Acquiring the data using a parameter fit from FCS curves, we were able to get the definite number of molecules in the confined volume,  $N = 5.19 \pm 1.615$ . Since background noise is not considered in the theoretical relation, this background noise (generated from the PDMS gasket, the impurities in the solution or the buffer itself) is possibly contributing to the number difference between the theoretical expectation and the real experimental values. In addition, photon bursts from outside of the  $e^{-2}$  volume still contribute to the molecular number since the laser beam creates a Gaussian intensity profile. Curves using the diffusion/flow model showed a good linear relationship between the applied electric field and the flow speed of the analyte (Figure 5). We were also able to verify from the fits that the one dimensional FCS model was adequate because of the confinement effect of the nanochannels. In Figure S5, all three FCS graphs showed good agreements between the obtained data and the model fit from Equation (1) with a high correlation. Analyte velocities as high as  $1.4 \text{ mm/sec}$  were obtained corresponding to an average residency time in the focal volume of approximately  $380 \mu\text{s}$ .

## 4. Conclusion

In summary, while electrospinning has been considered a random process for forming nanoscale fibers, here we represent post-processing approaches for nanofibers in order to reduce the mean value of the electrospun nanofiber dimension. We introduce two straightforward methods (with heat and with oxygen plasma) for further reduction of backbone nanofibers and confirm their stable applications to electrospun fibers. This is an important advancement in that it allows one to fabricate a wider array of more useful nanofluidic device without complicating the fabrication process. Successful manipulation of single molecules such as T4 DNA elongation and FCS studies in the nanochannels was demonstrated. We envision that this form of nanofabrication could robustly facilitate the electrospinning process for smaller nanofiber formation and the rapid prototyping of nanofluidic devices.

## Supporting Information

Supporting Information is available from the Wiley Online Library or from the author.

## Acknowledgements

The authors thank Drs. Scott Verbridge, David Czaplowski and Jin-Kyun Lee for helpful discussions of electrospinning. The authors also acknowledge use of the Keck SEM administered by the NSF-MRSEC at Cornell; Malcolm Thomas, facility manager. The authors

acknowledge funding from and access to the facilities of the Nanobiotechnology Center (NBTC), an STC Program of the National Science Foundation under Agreement no. ECS-9876771. The authors also appreciate access and use of the Cornell Nanoscale Science and Technology Facility (a member of the National Nanofabrication Users Network), which is supported by the National Science Foundation under grant ECS-9731293.

- 
- [1] J. H. Lee, B. D. Cosgrove, D. A. Lauffenburger, J. Han, *J. Am. Chem. Soc.* **2009**, *131*, 10340–10341.
- [2] J. H. Lee, Y.-A. Song, S. R. Tannenbaum, J. Han, *Anal. Chem.* **2008**, *80*, 3198–3204.
- [3] X. Liang, S. Y. Chou, *Nano Lett.* **2008**, *8*, 1472–1476.
- [4] M. Zwolak, M. Di Ventra, *Nano Lett.* **2005**, *5*, 421–424.
- [5] J. Han, H. G. Craighead, *Science* **2000**, *288*, 1026–1029.
- [6] S.-m. Park, Y. S. Huh, H. G. Craighead, D. Erickson, *Proc. Natl. Acad. Sci. USA* **2009**, *106*, 15549–15554.
- [7] R. H. Austin, *HFPJ* **2008**, *2*, 262–265.
- [8] R. Austin, *Nat. Nanotechnol.* **2007**, *2*, 79–80.
- [9] J. C. T. Eijkel, A. v. d. Berg, *Microfluid. Nanofluid.* **2005**, *1*, 249–267.
- [10] P. Abgrall, N. T. Nguyen, *Anal. Chem.* **2008**, *80*, 2326–2341.
- [11] S. Chung, J. H. Lee, M.-W. Moon, J. Han, R. D. Kamm, *Adv. Mater.* **2008**, *20*, 3011–3016.
- [12] D. Huh, K. L. Mills, X. Zhu, M. A. Burns, M. D. Thouless, S. Takayama, *Nat. Mater.* **2007**, *6*, 424–428.
- [13] L. M. Bellan, E. A. Strychalski, H. G. Craighead, *J. Vac. Sci. Technol., B* **2008**, *26*, 1728–1731.
- [14] D. A. Czaplewski, J. Kameoka, R. Mathers, G. W. Coates, H. G. Craighead, *Appl. Phys. Lett.* **2003**, *83*, 4836–4838.
- [15] S. S. Verbridge, J. B. Edel, S. M. Stavis, J. M. Moran-Mirabal, S. D. Allen, G. Coates, H. G. Craighead, *J. Appl. Phys.* **2005**, *97*, 124317.
- [16] M. Wang, N. Jing, B. S. Chi, J. Kameoka, C.-K. Chou, M.-C. Hung, K.-A. Chang, *Appl. Phys. Lett.* **2006**, *88*, 033106.
- [17] N. L. Nerurkar, B. M. Baker, S. Sen, E. E. Wible, D. M. Elliott, R. L. Mauck, *Nat. Mater.* **2009**, *8*, 986–992.
- [18] L. M. Bellan, J. D. Cross, E. A. Strychalski, J. Moran-Mirabal, H. G. Craighead, *Nano Lett.* **2006**, *6*, 2526–2530.
- [19] K. C. Krogman, J. L. Lowery, N. S. Zacharia, G. C. Rutledge, P. T. Hammond *Nat. Mater.* **2009**, *8*, 512–518.
- [20] P. Y. W. Dankers, M. C. Harmsen, L. A. Brouwer, M. J. A. Van Luyn, E. W. Meijer, *Nat. Mater.* **2005**, *4*, 568–574.
- [21] L. M. Bellan, S. P. Singh, P. W. Henderson, T. J. Porri, H. G. Craighead, J. A. Spector, *Soft Matter* **2009**, *5*, 1354–1357.
- [22] D. Bin, E. S. Meghan, E. W. Gary, *Small* **2009**, *5*, 1508–1512.
- [23] M. Foquet, J. Korylch, W. R. Zipfel, W. W. Webb, H. G. Craighead *Anal. Chem.* **2004**, *76*, 1618–1626.
- [24] D. R. Moore, M. Cheng, E. B. Lobkovsky, G. W. Coates, *J. Am. Chem. Soc.* **2003**, *125*, 11911–11924.
- [25] M. Cheng, A. B. Attygalle, E. B. Lobkovsky, G. W. Coates, *J. Am. Chem. Soc.* **1999**, *121*, 11583–11584.
- [26] M. H. Moses, S. Michael, R. Gregory, P. B. Michael, *Phys. Fluids* **2001**, *13*, 2201–2220.
- [27] M. M. Hohman, M. Shin, G. Rutledge, M. P. Brenner, *Phys. Fluids* **2001**, *13*, 2221–2236.
- [28] J. Kameoka, R. Orth, Y. Yang, D. Czaplewski, R. Mathers, G. W. Coates, H. G. Craighead, *Nanotechnology* **2003**, *14*, 1124–1129.
- [29] J. T. Mannion, C. H. Reccius, J. D. Cross, H. G. Craighead, *Biophys. J.* **2006**, *90*, 4538–4545.
- [30] H. Blom, A. Chmyrov, K. Hassler, L. M. Davis, J. Widengren, *J. Phys. Chem. A* **2009**, *113*, 5554–5566.
- [31] G. N. Taylor, T. M. Wolf *Polym. Eng. Sci.* **1980**, *20*, 1087–1092.
- [32] M. A. Hartney, D. W. Hess, D. S. Soane, *J. Vac. Sci. Technol., B* **1989**, *7*, 1–13.
- [33] J. O. Tegenfeldt, C. Prinz, H. Cao, S. Chou, W. W. Reisner, R. Riehn, Y. M. Wang, E. C. Cox, J. C. Sturm, P. Silberzan, R. H. Austin, *Proc. Natl. Acad. Sci. USA* **2004**, *101*, 10979–10983.

Received: May 24, 2010

Published online: September 27, 2010